Sustainable Energy, Grids and Networks 16 (2018) 126–135

Contents lists available at ScienceDirect

Sustainable Energy, Grids and Networks

journal homepage: www.elsevier.com/locate/segan

Dynamic Thévenin equivalent and reduced network models for PMU-based power system voltage stability analysis

Ali Bidadfar [a,*], Hossein Hooshyar [b,1], Luigi Vanfretti [b,*,1]

[a] Technical University of Denmark—DTU, Denmark
[b] Rensselaer Polytechnic Institute, Troy, NY, USA

ARTICLE INFO

Article history:
Received 8 January 2018
Received in revised form 17 April 2018
Accepted 4 July 2018
Available online 11 July 2018

Keywords:
Voltage stability
PMU
Reduced network model

ABSTRACT

Measurement-based real-time voltage stability assessment methods typically use a Thévenin Equivalent (TE) model. The TE is computed under the assumption that all generators and loads seen from an individual load-bus are constant during the time-window when measurements are obtained. This assumption does not hold in actual power systems. In fact, load changes at other load-buses result in variations on the voltage of a single-port equivalent model of the power system as seen from a load-bus. To consider these variations, this paper uses an interpolation method to develop a dynamic TE model from synchrophasor measurements, which is suitable for measurement-based real-time voltage stability assessment. In addition, a reduced network model is proposed to separate and quantify the impact of other loads and generators on the voltage stability of an interested load-bus in networks without full observability. The proposed method has been assessed through various simulation scenarios, and illustrated using actual field measurements.

1. Introduction

The deployment of synchronized phasor measurement units (PMUs) aims to assist power system operators to access large quantities of high-resolution, time-synchronized measurement data [1]. One of the uses of these data (i.e. application) is real-time monitoring, which is becoming crucially important for today's power systems as they are experiencing challenging operating conditions.

One key application of real-time monitoring is voltage stability assessment using synchrophasors [2–10]. Most studies in this area use a Thévenin equivalent (TE) circuit to represent the entire power system seen from an individual load-bus as a single-port model. Once the TE circuit is estimated, using the impedance matching concept, the voltage stability margin can also be estimated. The assumption of the TE model is that all generation and load seen from an individual load-bus do not experience variations during the period of time (one sampling window) when the PMU measurements are obtained. However, as discussed in [11], this assumption is not valid in actual power systems as other loads have coupling effects on the single-port model. In [2,6], and [10], it is claimed that by using two consecutive measurement snapshots the TE model can be computed assuming that within the time interval when the measurements are obtained, generation and other loads implicitly remain constant. While this assumption might be satisfied during normal operating conditions (quasi steady-state), the result of applying them when there are some variations (caused by loads, generators, or control actions) in the system will make the TE circuit parameters uncertain and sensitive to the system's response and noise.

In [11], an additional impedance is used to represent the coupling effects of other loads, and assumes that all loads in the system increase at the same rate, which is not the case in all operating conditions. This method was modified in [4] by introducing a correction factor generated from two consecutive PMU snapshots. As a result, the TE parameters are updated every two PMU snapshots.

The fact is that power systems undergo continuous variations, and thus, the TE impedance seen from a particular bus cannot be fully represented by a constant value. Consequently, the TE impedance needs to be represented using a dynamic impedance, which can be described using the rate of change of voltage with respect to current. Such dynamic impedance will vary in response to changes in generation, loads, or control actions of devices in the system; such as on-load tap changer, over excitation limiter, and others.

* Corresponding authors.
E-mail addresses: abid@dtu.dk (A. Bidadfar), hooshh@rpi.edu (H. Hooshyar), vanfrl@rpi.edu (L. Vanfretti).

[1] The work of L. Vanfretti and H. Hooshyar was supported in part by the Engineering Research Center Program of the National Science Foundation and the Department of Energy under Award EEC-1041877 and in part by the CURENT Industry Partnership Program.

https://doi.org/10.1016/j.segan.2018.07.002
2352-4677/

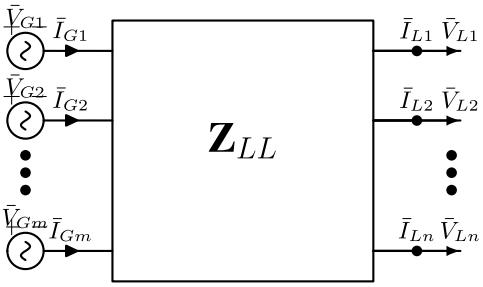

Fig. 1. Multi-port model of a power system.

This paper uses a method where dynamic TE impedance seen from an individual load-bus are estimated using polynomial interpolation applied on PMU-data snapshots. Unlike other methods, [2–10], the output of the proposed method is a complex-valued array representing TE impedance for singular measurement snapshot within a sampling window (in other methods, a single value is calculated for entire sampling window). In this method, first, the voltage and current phasors from a PMU in a window are parceled. Then, by using polynomial interpolation, the voltage phasors are modeled as a function of the load current. Using the obtained function, a dynamic impedance is computed by differentiating the voltage with respect to the current similar to those presented in [12,13]. However, to understand and quantify the impact of other loads or generators within a cut-set area [14] where all buses are not observable a reduced network model (RNM) is proposed in this paper. A dynamic instability index (ISI) can be calculated using estimated dynamic TE impedance indicating how close a power system is to voltage collapse point.

The paper is organized as follows. In Section 2, the coupled single-port model is presented. In Section 3, the interpolation technique applied to calculate the dynamic TE parameters is explained. Section 4 introduces the new RNM and shows how the coupling effect of other loads are computed. In Section 5, numerical analysis using real data as well as simulation results are provided. Conclusions are presented in Section 6.

2. Coupled single-port model

To derive the coupled single-port model, a multi-port network model of the entire system is used (see Fig. 1 [11]). The model is built from the nodal equations, i.e. $I = YV$, where Y, I, and V are respectively the admittance matrix, injection current vector, and node voltage vector. This equation can be expanded as follows:

$$\begin{bmatrix} -I_L \\ 0 \\ I_G \end{bmatrix} = \begin{bmatrix} Y_{LL} & Y_{LT} & Y_{LG} \\ Y_{TL} & Y_{TT} & Y_{TG} \\ Y_{GL} & Y_{GT} & Y_{GG} \end{bmatrix} \begin{bmatrix} V_L \\ V_T \\ V_G \end{bmatrix} \tag{1}$$

where the subscripts L, T, and G stand for load, tie, and generation buses, respectively. By eliminating the tie buses, (1) can be restated as:

$$\begin{aligned} V_L &= E_{eq} - Z_{LL} I_L \\ E_{eq} &= Z_{LL} \left(Y_{LT} Y_{TT}^{-1} Y_{TG} - Y_{LG} \right) V_G \\ Z_{LL} &= \left(Y_{LL} - Y_{LT} Y_{TT}^{-1} Y_{TL} \right)^{-1}. \end{aligned} \tag{2}$$

For a particular load-bus i, (2) results in a coupled single-port model described as

$$\begin{aligned} \bar{V}_{Li} &= \bar{E}_{eq,i} - \bar{Z}_{LL,ii} \bar{I}_{Li} - \bar{E}_{cp,i} \\ \bar{E}_{cp,i} &= \sum_{j=1, i \neq j}^{n} \bar{Z}_{LL,ij} \bar{I}_{Lj} \end{aligned} \tag{3}$$

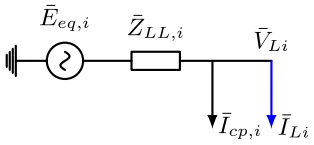

Fig. 2. Coupled single-port model of a power system seen from an individual load-bus.

where the $\bar{E}_{cp,i}$ represents the coupling impact of other loads on bus i. Alternatively, this coupling effect can be represented by an additional current source (5) or impedance (6) and (16) [11]. In this paper these two options are used. The concept of adding an extra impedance is used to justify how TE parameters seen from a particular load-bus i can be estimated by local PMU snapshots. Additionally, the concept of adding a current source is used to show how the coupling effects of other loads on TE impedance, consequently on voltage stability, of load-bus i can be quantified. This feature is further detailed in Section 4.2.

Only in a fully observable power system it is possible to retrieve all the variables in (3). As it may not be practical to install PMUs in all buses to make the entire network observable, voltages $\bar{E}_{eq,i}$ and $\bar{E}_{cp,i}$ cannot be readily available. Therefore, considerable work has been carried out to extract real-time TE parameters, $\bar{E}_{th}$ and $\bar{Z}_{th}$, from a local PMU measurements [2–9]. The validity of the TE model obtained using PMU measurements is questionable because the variation of other loads – reflected in the coupled voltage in (3) –are not included in the calculation of the TE parameters [11]. This is because, as shown in Fig. 3, the employed algorithms use two parcels of voltage and current measurements – each containing m samples – within a certain time interval (sampling window) to estimate one complex numbers, $\bar{Z}_{th}$, as the TE impedance. Whatever the variations are in the power system within the sampled window, the estimated impedance is always constant. Although, adjusting the sampling window length as well as window sliding (rolling) time can improve the result, the estimated TE impedance may experience some step changes when the window rolls forward. In this paper, the proposed algorithm estimates a complex vector, containing m complex numbers, as the TE impedance. Therefore, the system variations will be reflected in the estimated impedance. The proposed method is detailed in Section 3.

The pictorial representation of Eq. (3) is shown in Fig. 2, in which can be written as

$$\bar{I}_{cp,i} = \sum_{j=1, j \neq i}^{j=n} \frac{\bar{Z}_{LL,ij}}{\bar{Z}_{LL,ii}} \bar{I}_{Lj}. \tag{4}$$

To analyze the voltage stability at bus i using the impedance-matching criteria, the Thévenin impedance seen from an individual load-bus, $\bar{Z}_{th,i}$, must be known. The KVL equation of Fig. 2 can be written as

$$-\bar{E}_{eq,i} + \bar{Z}_{LL,ii} \left(\bar{I}_{Li} + \bar{I}_{cp,i} \right) = -\bar{V}_{Li}, \tag{5}$$

where it is clear the if $\bar{I}_{cp,i}$ is constant or it is linearly correlated to $\bar{I}_{Li}$, the (5) can be restated as a KVL equation in a TE circuit whose TE parameters can be estimated from $\bar{V}_{Li}$ and $\bar{I}_{Li}$ measurements. This has been carried out in [6] using the nonlinear least squares (NLS) method to derive (constant) TE parameters. However, note that the TE parameters can be constant only when there is a linear relation between the voltage, $\bar{V}_{Li}$, and the load current, $\bar{I}_{Li}$, of the individual load-bus. As mentioned before, such assumption is not valid for nonlinear power system behavior. Section 3 shows how (5) can be used to determine a dynamic Thévenin impedance to consider nonlinearity between the voltage and load current of an individual load-bus.

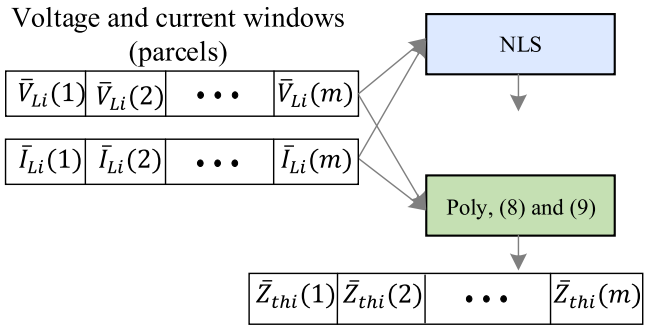

Fig. 3. From m snapshots of voltage and current phasors, the NLS method estimates a single fixed complex number as TE impedance, however, the Poly method estimates a complex vector (with m components) as TE impedance.

3. Dynamic impedance calculation

Taking derivatives of the variables in (5) with respect to the current $\bar{I}_{Li}$, results in

$$-\frac{d\bar{E}_{eq,i}}{d\bar{I}_{Li}}+\bar{Z}_{LL,ii}\left(1+\frac{d\bar{I}_{cp,i}}{d\bar{I}_{Li}}\right)=-\frac{d\bar{V}_{Li}}{d\bar{I}_{Li}}. \tag{6}$$

The right-hand side of (6) resembles a dynamic TE impedance seen from bus i. This is, in fact, the impedance whose amplitude is equal to the amplitude of the load impedance at the voltage collapse point.

In a stable condition (prior to voltage collapse) the apparent power, $\bar{S}_{Li}$, increases when its current increases (by decreasing the load impedance). At the nose point (voltage collapse point) although the load current increases, the apparent power does not change [15]. This implies that at the nose point the load apparent power is not sensitive to its current. The mathematical expression for this phenomena is given as

$$\begin{aligned}\left|\frac{d\bar{S}_{Li}}{d\bar{I}^*_{Li}}\right|=0 \;&\Rightarrow\left|\bar{V}_{Li}\frac{d\bar{I}^*_{Li}}{d\bar{I}^*_{Li}}+\bar{I}^*_{Li}\frac{d\bar{V}_{Li}}{d\bar{I}^*_{Li}}\right|=0\\ &\Rightarrow\left|\frac{\bar{V}_{Li}}{\bar{I}^*_{Li}}\right|=\left|-\frac{d\bar{V}_{Li}}{d\bar{I}^*_{Li}}\right|=|\bar{Z}_{th,i}|\end{aligned} \tag{7}$$

where $\bar{I}^*_{Li}$ is the conjugate form of the load current. This equation can also be justified using the Tellegen's theorem [10].

In this paper, to obtain the derivative of $\bar{V}_{Li}$ with respect to $\bar{I}_{Li}$, the voltage must be expressed as a function of the current, i.e. $\bar{V}_{Li}=f\left(\bar{I}_{Li}\right)$. To derive such function from PMU voltage and current phasors, polynomial interpolation is used. The main reason for using polynomial interpolation is that the resulting polynomial has a simple structure and, thus, it is straightforward to compute its derivative. The polynomial form of the voltage snapshots can be written as

$$\bar{V}_{Li}(n)=\sum_{k=0}^{Deg}p_k\bar{I}^k_{Li}(n) \tag{8}$$

where the Deg is the degree of polynomial equation, and n is a snapshot's number within a sampling window with m snapshots (see Fig. 3). The coefficient p_k is obtained using the interpolation method [16]. The value of Deg is not fixed and it is obtained iteratively as explained in the Appendix.

Differentiating the voltage in (8) with respect to current, that represents the dynamic TE impedance, can be written as

$$-\bar{Z}_{th,i}(n)=\frac{d\bar{V}_{Li}(n)}{d\bar{I}_{Li}(n)}=\sum_{k=1}^{Deg}k.p_k\bar{I}^{k-1}_{Li}(n). \tag{9}$$

4. A reduced network model to quantify load coupling effects

Based on the number of PMUs installed in a cut-set area, a reduced network model for the area is developed in order to quantify the effect of other loads and generators on the voltage stability of a load-bus. In other words, by obtaining the left-hand side terms of (6), the effect of other loads and generators on the dynamic impedance seen from the load-bus can be computed.

4.1. Reduced network model

Full observability is required to compute the coupling effects of all loads and generators on single-port models. However, in practice, making the whole system observable using PMUs is challenging due to several practical constraints [17]. Even if a power system has full observability this approach is particularly useful in practice, as the proposed method would be able to continue functioning under the loss of PMUs. Therefore, in this paper, an RNM is developed so that the number of buses in a cut-set area are reduced to observable buses, which include buses where PMUs are installed (PMU measured bus—PMUME) and those that are made observable from the measured currents and network parameters [18–20] (known as PMU-observable bus—PMUOB).

A PMUOB-bus is defined as a bus that is directly connected to a PMUME-bus via a series branch, such as a line or a transformer, whose current is measured by the PMU installed at the PMUME-bus. Therefore, the voltage of a seen-bus can be (linearly) estimated by the PMU-bus voltage and the voltage drop across the incident branch. In the proposed RNM methodology all unobservable buses are eliminated in such way that the voltage of observable buses are not affected.

To illustrate and explain the development of the RNM method, the IEEE 14-Bus test system, shown in Fig. 4(a), is considered to be a cut-set area that is connected to an external network (shown in a hatch square in the figure). It is assumed that the cut-set network is equipped with three PMUs at buses B1, B3, and B13. Bus B3 is a boundary bus between the cut-set area and the external network. Assuming that each PMU is able to measure the currents of its surrounding branches, the PMUOB-buses are B2, B4, B5, B6, B12, and B14. Accordingly, the unobservable buses would be B7, B8, B9, B10, and B11, which are indicated with gray color in Fig. 4(a). To reduce the network, first, the system's current–voltage relationship is considered

$$\begin{bmatrix}I'_{ob}\\ I_{un}\end{bmatrix}=\underbrace{\begin{bmatrix}Y_A & Y_B\\ Y_C & Y_D\end{bmatrix}}_{Y_{bus}}\begin{bmatrix}V_{ob}\\ V'_{un}\end{bmatrix} \tag{10}$$

where I'_{ob} is the vector of currents injected to observable buses. Note that although the voltage of PMUOB-buses can be estimated, their injected currents may be not. In other words, although I'_{ob} consists of currents injected to observable buses, some of its entries might be unknown. For instance, the voltage of buses B4, B6, and B14 in Fig. 4(a) can be estimated, but their injected currents can not. The matrix Y_{bus} in (10) is the system admittance matrix, the I_{un} is the vector of currents injected to unobservable buses, and V_{ob} and V'_{un} are the voltage vectors of observable and unobservable buses, respectively.

The goal is to keep only observable buses and remove unobservable ones in such a way that the voltage of observable buses remains unchanged. To achieve this goal, the loads and generators connected to unobservable buses are eliminated by setting their corresponding currents to zero, as shown in Fig. 4(b), i.e. $I_{un}=0$. Accordingly, the injected current to observable buses, and the voltage of unobservable buses, will be changed into I_{ob} and V_{un},

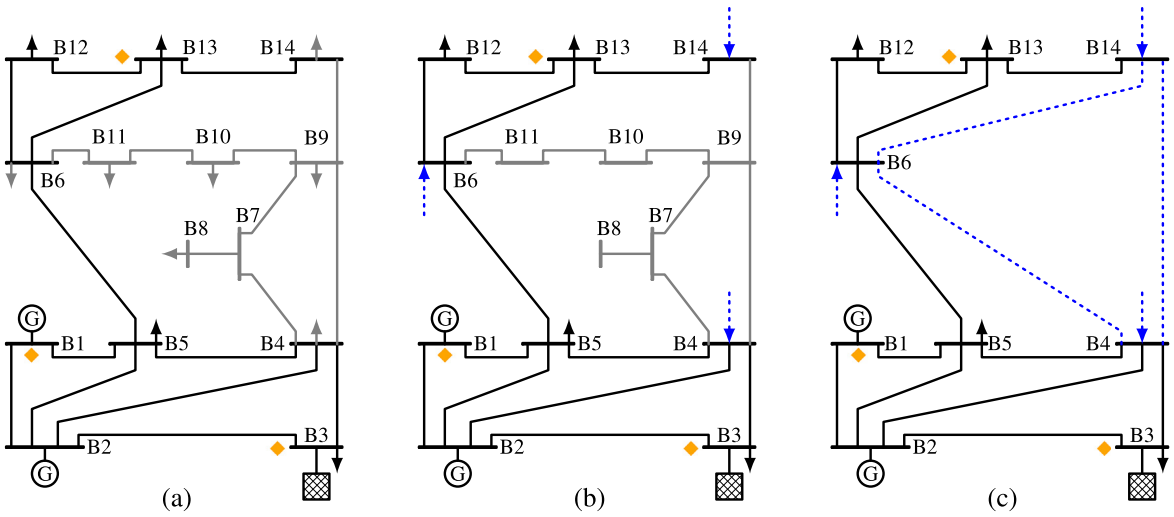

Fig. 4. IEEE 14-Bus test system presented as: (a) original model, (b) its equivalent, and (c) its RNM form. The sign ◆ indicates PMUME-bus. All unobservable components are shown in gray. The blue dotted arrows indicate calculated injected currents, and blue dotted lines are virtual lines that reflect the effect of the unobservable part of the network. (For interpretation of the references to color in this figure legend, the reader is referred to the web version of this article.)

respectively. Considering these modifications, Eq. (10) can be re-stated as

$$\begin{bmatrix} I_{ob} \\ 0 \end{bmatrix} = \begin{bmatrix} Y_A & Y_B \\ Y_C & Y_D \end{bmatrix} \begin{bmatrix} V_{ob} \\ V_{un} \end{bmatrix}. \tag{11}$$

This equation can be further simplified as

$$I_{ob} = Y_r V_{ob} \tag{12a}$$

$$Y_r = Y_A - Y_B Y_D^{-1} Y_C \tag{12b}$$

where Y_r is the admittance matrix of the reduced network model. As seen from (12), the reduced model relates all observable injected currents to observable buses. As a result, I_{ob} includes observable currents—shown as solid black arrows in Fig. 4—and a new 'equivalent' injected current for PMUOB buses—shown as blue dotted arrows in Fig. 4. The pictorial representation of (12a) and (12b) is illustrated in Fig. 4(c), where new lines and new injected currents, are shown with dotted blue lines, and are included to represent the effects of the unobservable part of the network. The admittance values of new lines are obtained from (12b), and the values of new injected currents are obtained from (12a). Therefore, it is possible to calculate all the newly injected currents shown in Fig. 4(c).

4.2. Coupling the effects of other loads on the voltage stability of the individual load-bus

By restating (12a) as $V = ZI$, where $Z = Y_r^{-1}$, $I = I_{ob}$, and $V = V_{ob}$, the voltage of a particular load-bus i can be written as

$$\bar{V}_{Li} = \bar{E}_{eq,Li} - \bar{Z}_{ii}\bar{I}_{Li} - \bar{E}_{cp,i} \tag{13}$$

$$\bar{E}_{cp,i} = \sum_{j=mo,\ i\neq j}^{no} \bar{Z}_{ij}\bar{I}_{Lj} \tag{14}$$

where *mo* and *no* are the number of observable generator and load buses, respectively. Note that (13) is similar to (3), but includes only observable buses. All variables in (13) and (14) can be obtained from (12). In (13), the effects of generation units, transmission lines and transformers, and other loads on the voltage of load-bus i are represented by $\bar{E}_{eq,Li}$, $\bar{Z}_{ii}\bar{I}_{Li}$, and $\bar{E}_{cp,i}$. However, two important points must be taken into account: first, as long as all generator buses are not observable, $\bar{E}_{cp,i}$ will not exclusively include the effects of other loads as the terms $\bar{E}_{cp,i}$ and $\bar{E}_{eq,Li}$ cannot be distinctly separated; second, depending on direction of the current, the external networks connected to boundary buses must be identified and represented as a lumped generator or load.

The voltage instability index (ISI) can be defined as [10,21–26]

$$\mathrm{ISI}_i = \frac{|\bar{Z}_{th,i}|}{|\bar{V}_{Li}/\bar{I}_{Li}|} \tag{15}$$

where the index varies from 0 to 1 as the system moves from stable to unstable. Note that the TE impedance in (15), $\bar{Z}_{th,i}$, is defined as a dynamic impedance in (9). From (15), it is possible to analyze how other loads and generation units can impact the voltage stability of an individual load-bus in two different ways: first, by affecting V_{Li}; and second, by changing the TE impedance seen from the individual load-bus. The first has a larger effect during stressed conditions, because the voltage magnitude of load buses are kept relatively constant and above 0.95 per-unit during steady state operation. However, the second is prevalent during all operational conditions and must be identified through (6). As indicated in (6), the TE impedance, $\bar{Z}_{th,i}$, is influenced by both $\bar{E}_{eq,i}$ and $\bar{I}_{cp,i}$, which respectively represent the effect of other generation units and loads. In addition, if fast AVR operation is assumed, the term $d\bar{E}_{eq,i}/d\bar{I}_{Li}$ in (6) may be neglected.

The index estimated in (15) is similar to the one proposed in [27] (called SDC). However, the SDC is a transient index which uses two consecutive measurements, while the ISI uses a parcel of measurements of m samples, which makes it numerically stable.

To study the effect of $I_{cp,i}$ on TE impedance, $\bar{Z}_{th,i}$, the currents of other loads, i.e. $\bar{I}_{Lj}$, should be defined as functions of $\bar{I}_{Li}$ by applying polynomial interpolation, as defined in (8). By using (6), the TE impedance can be written as

$$\frac{d\bar{V}_{Li}}{d\bar{I}_{Li}} = -\bar{Z}_{ii} - \bar{Z}_{cp,i} = -\bar{Z}_{th,i} \tag{16a}$$

$$\bar{Z}_{cp,i} = \sum_{j=mo,\ i\neq j}^{no} \bar{Z}_{ij}\frac{d\bar{I}_{Lj}}{d\bar{I}_{Li}} \tag{16b}$$

The effects of other loads on the voltage drop as well as on voltage stability of bus i can be observed from (13) as an extra voltage source and from (16a) as an extra impedance, respectively. In other words, by introducing $\bar{E}_{cp,i}$ in (13), and $\bar{Z}_{cp,i}$ in (16a), the impact of other loads on the voltage stability of bus i can be captured. To quantify this coupling effect, the derivative term in (16b) is estimated using a polynomial expression. To do so, each of observable

current $\bar{I}_{Lj}$ should be stated as a polynomial function of the load current $\bar{I}_{Li}$. For a sampling window with m components, this is done as

$$\bar{I}_{Lj}(n) = \sum_{k=0}^{Deg} q_k \bar{I}_{Li}^{k}(n) \tag{17}$$

where the k is determined similarly as for (8), and q_k is obtained using the interpolation method. Therefore, similar to estimating the TE impedance in (9), the coupling impedance between bus j and i can also be estimated by taking derivative of (17) with respect to $\bar{I}_{Li}$.

$$\bar{Z}_{cp,ji}(n) = \bar{Z}_{ij} \frac{d\bar{I}_{Lj}(n)}{d\bar{I}_{Li}(n)} = \bar{Z}_{ij} \sum_{k=1}^{Deg} k.q_k \bar{I}_{Li}^{k-1}(n) \tag{18}$$

This impedance indicates the effect of load j on the TE impedance seen from load-bus i. Consequently, the effect of load j on the voltage stability of load-bus i can be estimated as

$$\mathrm{ISI}_{cp,ji} = \frac{\left|\bar{Z}_{cp,ji}\right|}{\left|\bar{V}_{Li}/\bar{I}_{Li}\right|} \tag{19}$$

5. Numerical analyses

This section provides numerical analyses on the proposed method. It includes the calculation of TE impedance and stability indexes using real PMU data from the Nordic power system, and the calculation of TE impedance and stability indexes computed from quasi-steady-state simulations of the IEEE 14-bus test system and full dynamic simulations (i.e. "transient stability"-type) of Nordic 32-bus test system under different conditions.

5.1. Real PMU measurements from the Nordic power system

In order to show how the proposed method can be applied to real data, PMU measurements obtained during an event in the northern part of the Nordic grid are analyzed in this section. The data was measured at bus that was close to experience voltage collapse on January 29th, 2010 [28]. Fig. 5 shows the PMU data of the bus voltage and the line current connected to it. As seen from this figure, the voltage magnitude started to drop at the 35th minute. Subsequently, one of the transmission lines near the measured bus was disconnected at the 37th min. An OLTC was activated to step up the voltage level at $t = 38.5$ min and $t = 42$ min, respectively. However, because the voltage was below allowed operational limits, a large industrial load, located 160 km away from its feeding substation, was manually disconnected to prevent a voltage collapse.

The TE impedance of the network seen from the PMU was calculated using three methods and results are shown in Fig. 6. As shown in the figure, the dynamic Z_{th} obtained from the proposed method, with a window of one minute, has been compared with the Z_{th} obtained using NLS estimation [3] with a window of 10 s (referred as NLS1), and NLS estimation with a window of 1 min (referred as NLS2). Note that due to the presence of noise in the PMU data, it was not possible to use neither the NLS method with smaller window of data nor the two-samples method to obtain robust outputs (high variability). The proposed polynomial method is used with a varying polynomial degree. Algorithm 1 in the Appendix gave a polynomial degree that did not increase from $Deg = 2$ in all windows. Fig. 7 compares the voltage instability indexes calculated using the TE impedances shown in Fig. 6. As indicated by Figs. 6 and 7, the proposed polynomial method (dynamic TE impedance) provides smoother results (especially compared to NLS1) as it mitigates the impact of measurement noise efficiently.

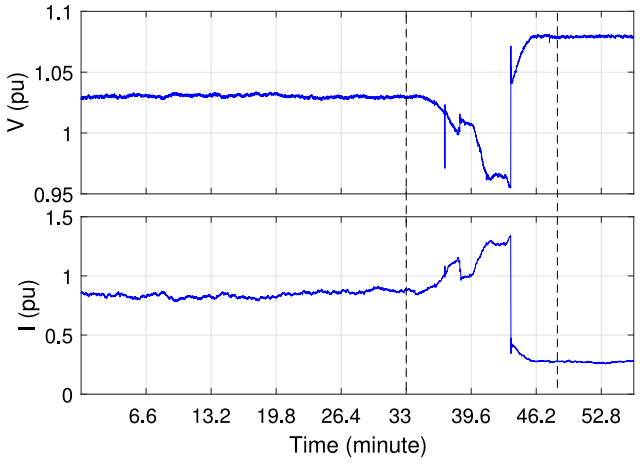

Fig. 5. PMU measurements of the bus voltage and line current magnitudes in the Nordic grid during an event in 2010.

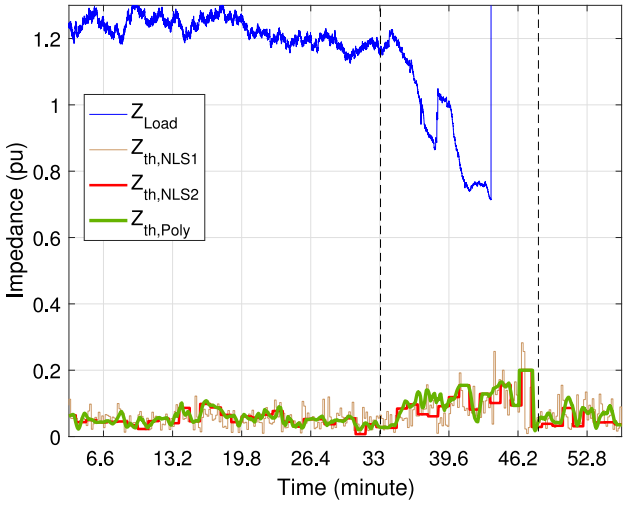

Fig. 6. TE impedance calculated using different methods.

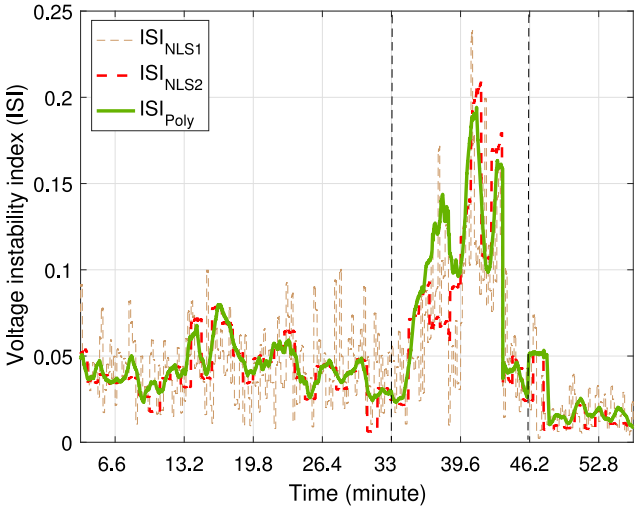

Fig. 7. Voltage instability index calculated using different methods.

In addition, results from the proposed method show consistency with the measured data. For example, the ISI calculated by the

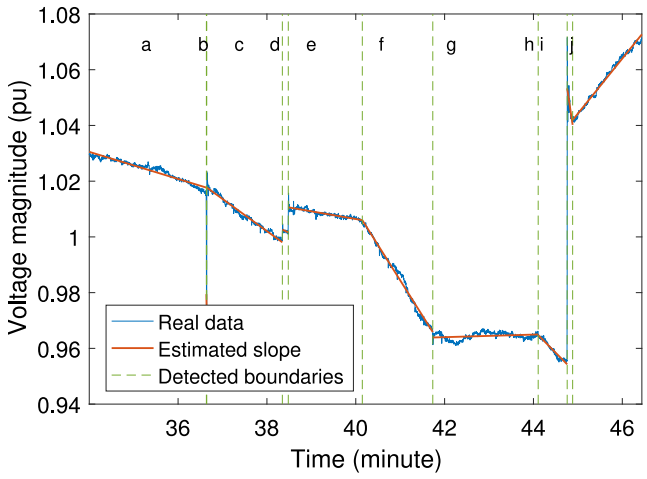

Fig. 8. Detection of significant changes, including step changes, in voltage magnitude when system is approaching the voltage collapse point. The letters *a* to *j* correspond to different operating condition shown in Fig. 9.

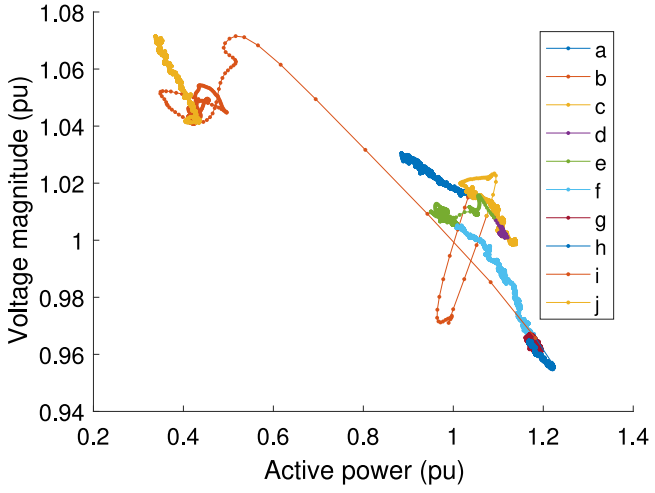

Fig. 9. Power-voltage (PV) curve of real data when system is approaching the voltage collapse point. The letters *a* to *j* correspond to different operating conditions.

proposed method increases at $t = 37$ s (when the transmission line disconnects) whereas that of the NLS2 decreases.

Note that the reduced network model has not been used for this study, because neither the network model nor more than one PMUs' data are available.

Any contingencies and sudden changes in power systems result in step changes and shift in the system operating point. In order to detect these changes, transients and also distinguish the boundary between two operation points, this paper uses PELT (Pruned Exact Linear Time) algorithm [29]. The Fig. 8 shows how the different changes have been detected when the system is approaching the voltage collapse point. The letters *a* to *j* in Figs. 8 and 9 correspond to different operating conditions. The load shedding, tap-changer operation, and generator excitation current limitation are the cause of shifting from one operating point to another. For instance transition from *c* to *d*, and also from *d* to *e* has occurred because of tap changer action. A significant load shedding has caused transition for *h* to *i*.

5.2. IEEE 14-bus test system

To demonstrate how the TE parameters are calculated for a system with different load variations, it is assumed that the load-bus B13 in IEEE 14-bus test system, shown in Fig. 4a, is interested for voltage stability studies. Different scenarios have been simulated and the TE impedance seen from the individual load-bus is calculated using three different methods: the two-samples method (2S) [6,11], the NLS, and polynomial interpolation method (Poly). The window length for both the NLS and Poly methods is one minute. The simulations for IEEE 14-bus system are of quasi-steady-state type which makes the simulated phasor data noise-free and the TE impedance calculated using the two-samples method provides the best TE estimation, against which the TE impedances obtained from the other methods can be compared. In all scenarios, the apparent power of the load connected to B13 is increased until it approaches to the voltage instability point.

Notice that in all figures LDx stands for load number x, and the term "Effect of Bx" implies the variation effect of load at bus x in the dynamic TE impedance seen from bus B13. This effect is estimated using (18).

Scenario I- no load variation

In the first scenario, all loads other than B13 are kept constant, and the TE impedance is calculated using the three methods mentioned above. The results are shown in Fig. 10. As shown in the figure, the three methods give almost identical results. The degree for polynomial interpolation obtained using the algorithm in Appendix was 1 for all time windows.

Scenario II—all loads vary linearly

As another scenario, it is assumed that the power of all loads of the network, other than the one connected to B13, increase linearly by 1% (0.01 pu) per minute. The TE impedance seen from B13 was calculated and is shown in Fig. 11. In this scenario the proposed RNM methodology has been applied. It is assumed that the loads in gray in Fig. 4(a) are unobservable and their effects on the TE impedance seen from B13 are determined via buses B4, B6, and B14 (shown by dashed-lines in Fig. 11). Using (4) and (9), the effect of the load variation at other buses on the TE impedance seen from an interested bus depends on two factors: first, the distance between that bus and the interested bus, which is indicated by the impedance, $\bar{Z}_{LL.ij}$, and second, the size of the load current at that bus, which is represented by $\bar{I}_{Lj}$. For instance, the variation of the load connected at bus B14 has the highest effect on TE impedance seen from the bus B13. This is because the bus B14 is too close to bus B13 (see Fig. 12).

Scenario III—different variations in other loads

In the last scenario, different types of variations are considered for different loads and their effects on the TE impedance of B13 are computed. These variations aim to replicate the behavior of more complex loads found in real power systems. The types of variations considered for the power of different loads are shown in Fig. 13. Fig. 14 shows the calculated TE impedance seen from bus B13 with different methods. In addition, the figure shows the effects caused by the variations of other loads on TE impedance of bus B13. The polynomial degree for interpolation computed from the Algorithm 1 in this scenario is 7. As seen from Fig. 14, the NLS method shows a noticeable error in the calculation of the TE impedance, and consequently, the voltage instability index especially when system approaches to the voltage instability point. The voltage instability index and the contribution of other loads' variations to this index are shown in Fig. 15. As shown in Figs. 14 and 15 for the same sampling window (60 s), the NLS method is unable to follow system variations, while the Poly method has a better response. In order to improve the NLS method, its sampling window length and window rolling rate can be updated. However, such effort is not needed for the Poly method.

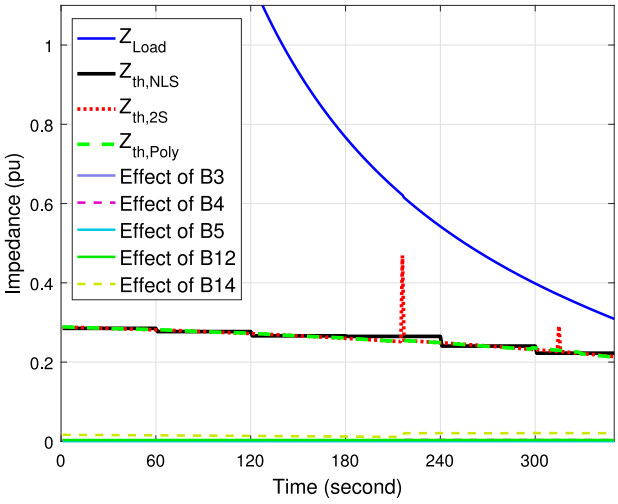

Fig. 10. Load and TE impedance magnitude seen from bus B13 of IEEE 14-bus system when other loads than load 13 are not varying.

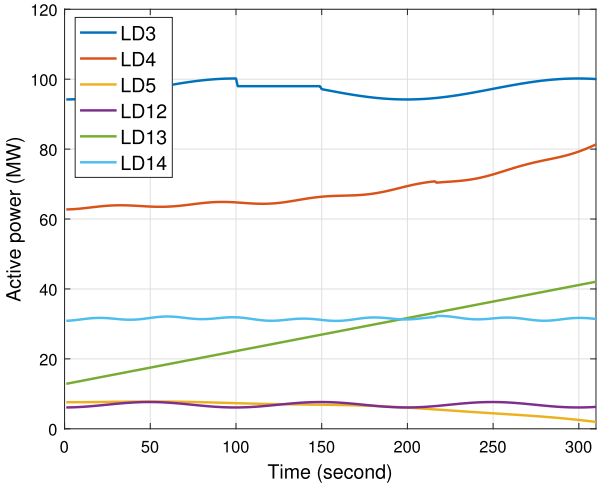

Fig. 13. Active power of Loads on different buses of IEEE 14-bus system are varying haphazardly.

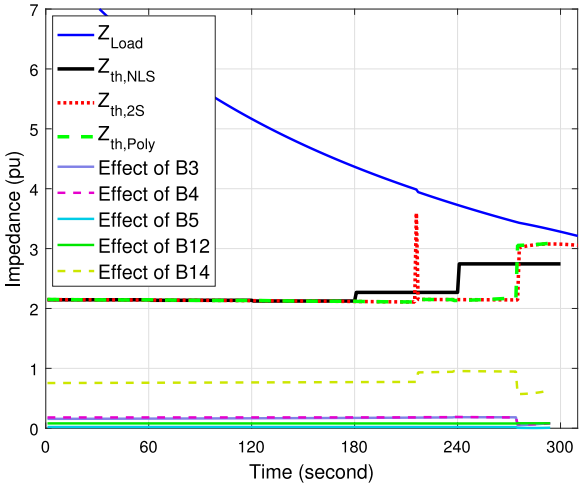

Fig. 11. Load and TE impedance magnitude seen from bus B13 of IEEE 14-bus system when other loads are all varying linearly.

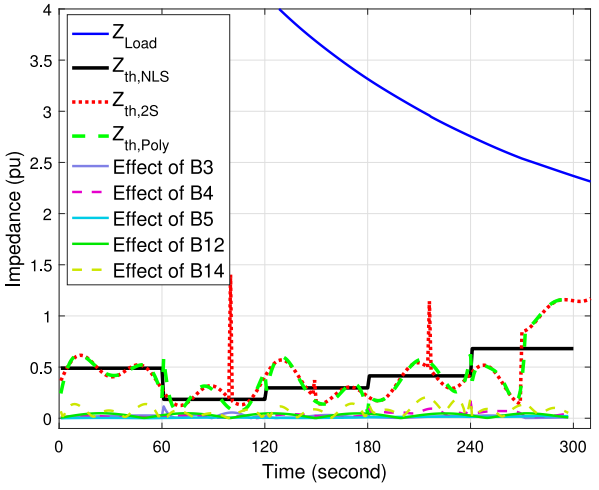

Fig. 14. Load and TE impedance magnitude seen from bus B13 of IEEE 14-bus system when other loads are varying haphazardly as shown in Fig. 13.

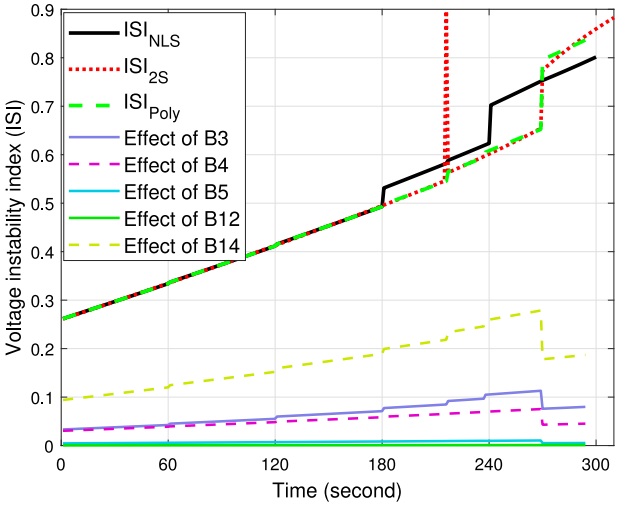

Fig. 12. ISI calculated for bus B13 of IEEE 14-bus system when other loads are all varying linearly.

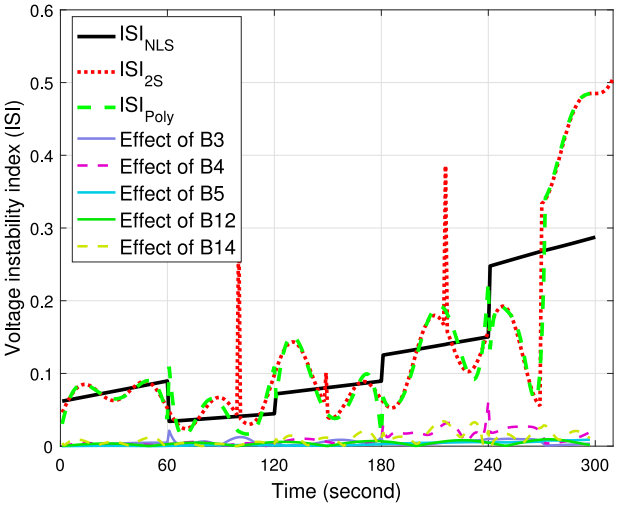

Fig. 15. ISI calculated for bus B13 of IEEE 14-bus system under the load variations illustrated in Fig. 13.

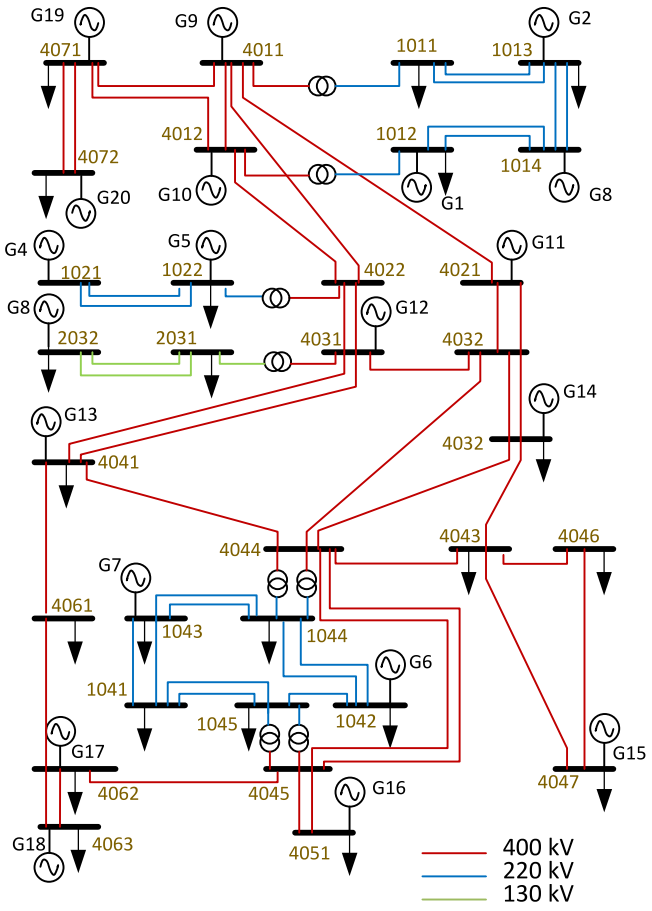

Fig. 16. Single-line diagram of the Nordic 32-bus test system.

5.3. Nordic 32-bus dynamic model

To test the proposed method on a larger and more complex model that is relevant for voltage stability assessment, the Nordic 32-bus test system is used [30]. The single-line diagram of this test system is shown in Fig. 16. The simulation has run in the time-domain, and loads at bus B1041 and B1045 are increased as shown in Fig. 17. The system becomes voltage-unstable at bus B1041 at $t = 4.7$ min. as shown in Fig. 18. As the system approaches the voltage instability point, the excitation current as well as speed of system generators are affected as shown in Fig. 19.

The TE impedance seen from bus B1041 has been estimated by different methods and shown in Fig. 20. In this simulation the reduced network model is used to estimate the effects of other loads' variation in the TE impedance seen from B1041. These effects which are shown in Fig. 20 depend on the system impedance $\bar{Z}_{LL,ii}$ and deviation of other loads current with respect to interested load's current as shown by (6). In Fig. 20 it is shown that the load at bus B1045 has highest effect on the TE impedance seen from B1041 after $t = 2$ min. This can be justified by observing the current magnitude in Fig. 21 which clearly shows the load current at bus B1045 starts increasing after $t = 2$ min.

The ISI calculated by different methods for bus B1041 is shown in Fig. 22 in which a voltage instability detected at $t = 4.7$ min. The stability margin in ISI depends on two factors: maximum allowed voltage drop and minimum loading margin. According to the PV curve, voltage instability index, and voltage magnitude of bus B1041, if the loading margin is assumed to be 30%, and maximum voltage drop is 6%, the stability margin on ISI would be around 0.81,

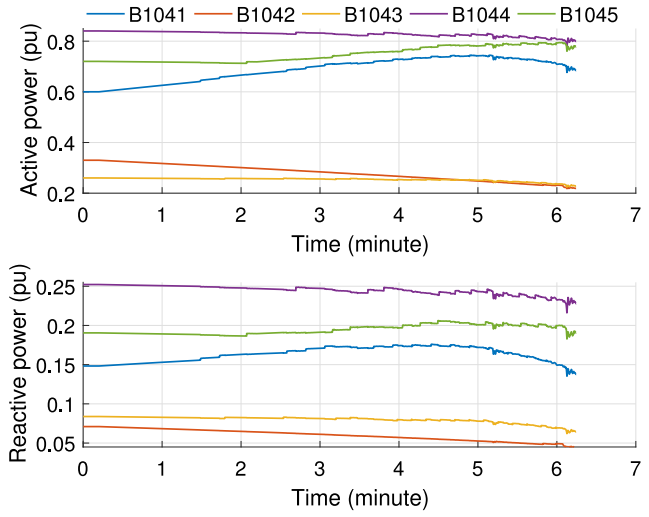

Fig. 17. Active and reactive power of observable load buses in Nordic 32-bus test system.

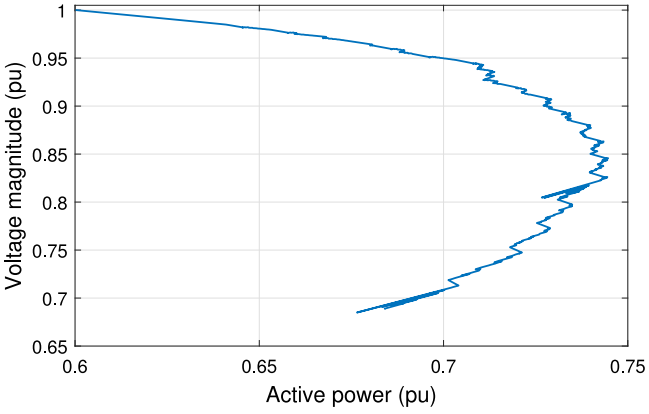

Fig. 18. Power-voltage (PV) curve of the load connected at bus B1041 in Nordic 32-bus test system.

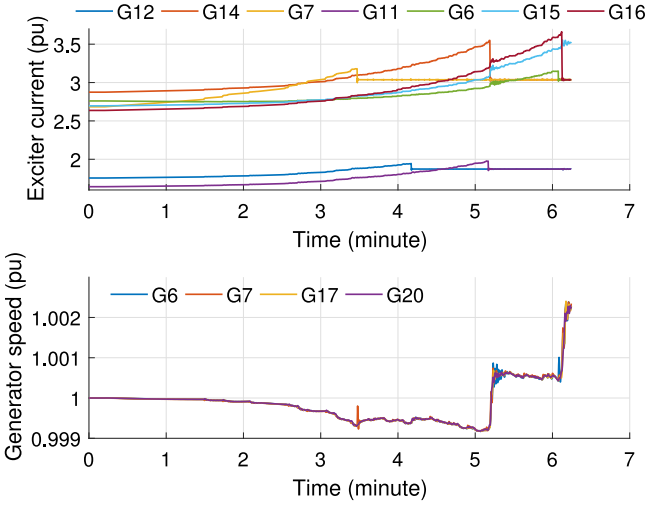

Fig. 19. Excitation current and speed of some generators of Nordic 32-bus system where it approaches to voltage instability point in bus B1041.

which means the ISI range from 0 to .81 indicates secure operation region.

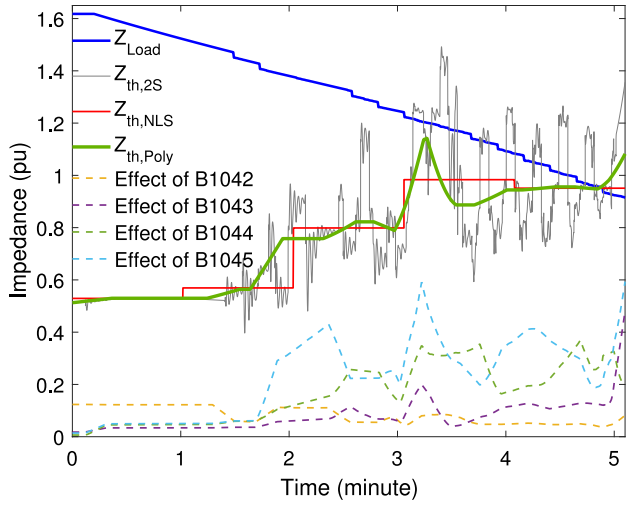

Fig. 20. Load and TE impedance magnitude seen from bus B1041. Contribution of other loads' variation in the TE impedance are shown with dashed-lines.

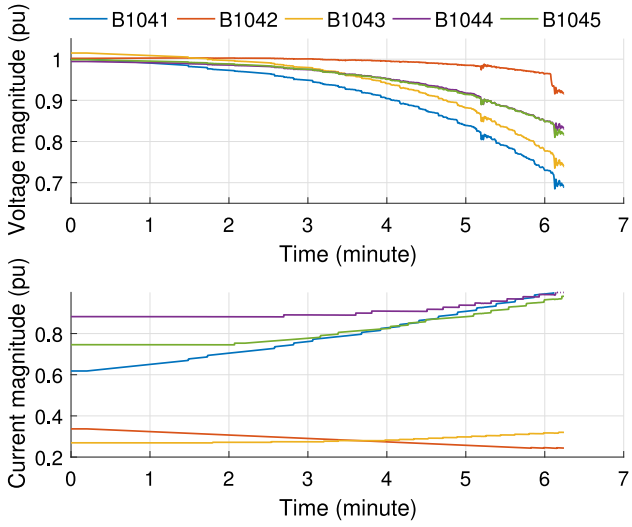

Fig. 21. Voltage and current magnitude of observable load buses in Nordic 32-bus system.

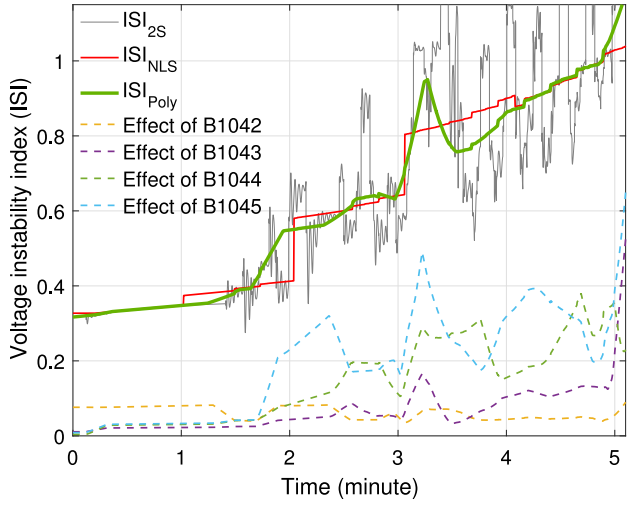

Fig. 22. ISI calculated by different methods for bus B1041 of Nordic 32-bus system.

6. Conclusions

This paper proposed a polynomial interpolation method to calculate the TE impedance of a power network seen from a load bus that can be used for real-time voltage stability monitoring. Using the proposed interpolation method, the voltage of a load-bus can be described as a polynomial function with respect to injected current from that bus. The derivative of this polynomial reflects the dynamic TE impedance seen from the bus. The computed impedance, which is a vector rather than a scalar, can take into account the effect of nonlinear variations of other loads. Moreover, by using the interpolation approach on other observable load currents, it was shown that it is possible to quantify the effect of load variations at other buses on the interested load-bus TE impedance.

In addition, the paper takes into account the fact that in real power systems all measured buses are not necessarily equipped with PMUs. To address this issue, this paper considers the network under study as a cut-set area within a power system. Under such conditions, a reduced network model and its computation were proposed. The approach allows to quantify the effect of load variations at other buses on the TE impedance seen from an interested load-bus, and consequently, on the voltage instability index.

Appendix. - Algorithm 1: Polynomial Degree Computation

The value of *Deg* in (8) is obtained iteratively using following algorithm

$\epsilon = 10^{-4}$; polynomial fit tolerance
$Deg_{max} = 8$
for *Deg*=1:Deg_{max} **do**
  Execute the polynomial interpolation algorithm for (8) and obtain the coefficients p_k
  $\bar{V}_{Li}^{m} = \sum_{k=0}^{Deg} p_k \bar{I}_{Li}^{k}$
  if $\left|\bar{V}_{Li}^{m} - \bar{V}_{Li}\right| \leq \epsilon$ **then**
    Break the **for** loop
  end if
end for

References

[1] F.C. Sanchez, P.D.H. Hines, C.M. Danforth, Predicting critical transitions from time series synchrophasor data, IEEE Trans. Smart Grid 3 (4) (2012) 1832–1840.
[2] S.M. Abdelkader, D.J. Morrow, Online tracking of Thévenin equivalent parameters using PMU measurements, IEEE Trans. Power Syst. 27 (2) (2012) 975–983.
[3] S. Corsi, G., N. Taranto, A real-time voltage instability identification algorithm based on local phasor measurements, IEEE Trans. Power Syst. 23 (3) (2008) 1271–1279.
[4] J.H. Liu, C.C. Chu, Wide-area measurement-based voltage stability indicators by modified coupled single-port models, IEEE Trans. Power Syst. 29 (2) (2014) 756–764.
[5] B. Milosevic, M. Begovic, Voltage-stability protection and control using a wide-area network of phasor measurements, IEEE Trans. Power Syst. 18 (1) (2003) 121–127.
[6] K. Vu, M.M. Begovic, D. Novosel, M.M. Saha, Use of local measurements to estimate voltage-stability margin, IEEE Trans. Power Syst. 14 (3) (1999) 1029–1035.
[7] G. Verbic, F. Gubina, A new concept of voltage-collapse protection based on local phasors, IEEE Trans. Power Deliv. 19 (2) (2004) 576–581.
[8] H.Y. Su, C.W. Liu, Estimating the voltage stability margin using PMU measurements, IEEE Trans. Power Syst. 31 (4) (2016) 3221–3229.
[9] J. Lavenius, L. Vanfretti, G.N. Taranto, Performance assessment of PMU-based estimation methods of Thévenin equivalents for real-time voltage stability monitoring, in: IEEE 15th International Conference on Environment and Electrical Engineering, EEEIC, 2015, Rome, Italy.
[10] I. Smon, G. Verbic, F. Gubina, Local voltage-stability index using Tellegen's theorem, IEEE Trans. Power Syst. 21 (3) (2006) 1267–1275.
[11] Y. Wang, I.R. Pordanjani, W. Li, W. Xu, T. Chen, E. Vaahedi, J. Gurney, Voltage stability monitoring based on the concept of coupled single-port circuit, IEEE Trans. Power Syst. 26 (4) (2011) 2154–2163.

[12] P.L.,V. Prasanna, S.S. Kumar, K.S.,R. Anjaneyulu, A novel voltage stability index based on the polynomial estimation from voltage and current measurements, in: 16th National Power Systems Conference, 2010, Hyderabad, India.
[13] D.K. Rai, Maximum permissible loading and Static voltage stability limit of a power system using V-I polynomial, Int. J. Comput. Eng. Res. 2 (5) (2012) 1438–1442.
[14] I. Dobson, M. Parashar, A cutset area concept for phasor monitoring, in: IEEE PES General Meeting, 2010, Minnesota, USA.
[15] P. Kundur, Power System Stability and Control, McGraw-Hill, inc., New York, 1994.
[16] N.N. Vasiliev, O. Kanzheleva, Polynomial interpolation over the residue rings Zn, J. Math. Sci. 209 (6) (2015) 845–850.
[17] N. Kashyap, S. Werner, Y.R. Huang, T. Riihonen, System state estimation under incomplete PMU observability a reduced-order approach, IEEE J. Sel. Top. Sign. Proces. 8 (6) (2014) 1051–1062.
[18] L. Vanfretti, J.H. Chow, S. Sarawgi, B. Fardanesh, A phasor-data-based state estimator incorporating phase bias correction, IEEE Trans. Power Syst. 26 (1) (2011) 111–119.
[19] D. Gyllstrom, E. Rosensweig, J. Kurose, On the impact of pmu placement on observability and cross-validation, in: Proceedings of the 3rd International Conference on Future Energy Systems: Where Energy, Computing and Communication Meet, e-Energy '12, ACM, New York, NY, USA, 2012, pp. 20:1–20:10.
[20] S.G. Ghiocel, J.H. Chow, G. Stefopoulos, B. Fardanesh, D. Maragal, B. Blanchard, M. Razanousky, D.B. Bertagnolli, Phasor-measurement-based state estimation for synchrophasor data quality improvement and power transfer interface monitoring, IEEE Trans. Power Syst. 29 (2) (2014) 881–888.
[21] M. Begovic, B. Milosevic, D. Novosel, A novel method for voltage instability protection, in: Proceedings of the 35th Annual Hawaii International Conference on System Sciences, 2002, pp. 802–811.
[22] S. Massucco, S. Grillo, A. Pitto, F. Silvestro, Evaluation of some indices for voltage stability assessment, in: 2009 IEEE Bucharest PowerTech, 2009, pp. 1–8.
[23] A.F.B. Abidin, A. Mohamed, On the use of voltage stability index to prevent undesirable distance relay operation during voltage instability, in: 2010 9th International Conference on Environment and Electrical Engineering, 2010, pp. 384–387.
[24] M.H. Haque, A smart instrument for on-line monitoring of static voltage stability index using local measurements, in: 2013 IEEE Innovative Smart Grid Technologies-Asia (ISGT Asia), 2013, pp. 1–5.
[25] J. Zhang, M. Liu, Y. Yin, W. Lin, Q. Wang, L. Liu, Y. Shao, A transient voltage stability index based on critical equivalent impedance, in: 2014 International Conference on Power System Technology, 2014, pp. 25–29.
[26] D.T. Duong, K. Uhlen, G.N. Taranto, S. Løvlund, A comparative case study of online voltage instability monitoring, in: 2015 IEEE Eindhoven PowerTech, 2015, pp. 1–6.
[27] M. Parniani, M. Vanouni, A fast local index for online estimation of closeness to loadability limit, IEEE Trans. Power Syst. 25 (1) (2010) 584–585.
[28] R. Leelaruji, L. Vanfretti, K. Uhlen, J.O. Gjerde, Computing sensitivities from synchrophasor data for voltage stability monitoring and visualization, Int. Trans. Electr. Energ. Syst. 1 (25) (2014) 933–947.
[29] R. Killick, I.A. Eckley, Changepoint: an R package for changepoint analysis, J. Stat. Softw. 58 (3) (2014) 1–19.
[30] IEEE PES Task Force on Test Systems for Voltage Stability Analysis and Security Assessment, IEEE Power and Energy Society, 2015.